Title

New Zn(II) complexes with N2S2 Schiff base ligands. Experimental and theoretical studies of the role of Zn(II) in disulfide thiolate-exchange

Authors

Amirnasr, Mehdi
Bagheri, Maryam
Farrokhpour, Hossein
et al.

Publication Date

2014-03-01

DOI

10.1016/j.poly.2013.12.040

Peer reviewed

Polyhedron 71 (2014) 1–7

Contents lists available at ScienceDirect

Polyhedron

journal homepage: www.elsevier.com/locate/poly

New Zn(II) complexes with N_2S_2 Schiff base ligands. Experimental and theoretical studies of the role of Zn(II) in disulfide thiolate-exchange

Mehdi Amirnasr [a,*], Maryam Bagheri [a], Hossein Farrokhpour [a], Kurt Joβ Schenk [b], Kurt Mereiter [c], Peter C. Ford [d]

[a] Department of Chemistry, Isfahan University of Technology, Isfahan 84156-83111, Iran
[b] Laboratoire de Cristallographie, École Polytechnique Fédérale de Lausanne, Le Cubotron-521, Dorigny, CH-1015 Lausanne, Switzerland
[c] Faculty of Chemistry, Vienna University of Technology, Getreidemarkt 9/164SC, A-1060 Vienna, Austria
[d] Department of Chemistry and Biochemistry, University of California, Santa Barbara, CA 93106, USA

ARTICLE INFO

Article history:
Received 13 October 2013
Accepted 26 December 2013
Available online 9 January 2014

Keywords:
N_2S_2 Schiff base
Zn(II) complex
Disulfide bond cleavage
Crystal structure
Cyclic voltammetry

ABSTRACT

Described are the synthesis and characterization of two, potentially tetradentate, N_2S_2 Schiff-base ligands, containing a disulfide bond, N,N′-bis(3-phenylprop-2-en-1-ylidene)-2,2′-disulfanediyldianiline (**L**^{1}) and N,N′-bis(3,3-diphenylprop-2-en-1-ylidene)-2,2′-disulfanediyldianiline (**L**^{2}), and their reaction with Zn^{2+}. Surprisingly, both **L**^{1} and **L**^{2} undergo reductive disulfide bond scission upon reaction with Zn^{2+} in alcoholic media to give, under alcohol oxidation, the respective $Zn(NS)_2$ complexes $Zn(L^3)_2$ (**1**) and $Zn(L^4)_2$ (**2**), where the **L**^{3} and **L**^{4} are the respective bidentate thiolate-imine anions. The ligands **L**^{1} and **L**^{2} and the complexes **1** and **2** have been characterized spectroscopically, and the crystal and molecular structures of the two complexes have been determined by single crystal X-ray diffraction. The coordination geometry around Zn(II) centers in both complexes is a distorted tetrahedron. In addition, DFT calculations (B3LYP/LANL2DZ/6-311++G(d,p)) support the structure of **1**. Cyclic voltammetric studies demonstrate that Zn(II) shifts the reduction potential of the disulfide ligands **L**^{1} and **L**^{2} to less negative values thus making them more susceptible to reductive cleavage of the disulfide bond. The results of semi-empirical PM6 calculations offer key insight into the nature of the transition state for this reaction.

1. Introduction

Zinc, which is always present in the +2 oxidation state in organisms, plays a number of important roles in protein chemistry [1–5]. Examples include the interactions of the thiols of cysteine (Cys) residues with Zn^{2+} in various metallothioneins and zinc fingers [1,2]. Notably, since cysteine is redox active, although Zn^{2+} is not, zinc coordination environments with multiple thiol or thiolate ligands can be oxidized and then reduced again at the sulfur centers with concomitant release and binding of Zn^{2+} (Scheme 1) [6]. For example, in zinc fingers a thiol-disulfide exchange reaction can occur between a protein bearing small thiol-containing residues, such as glutathione, and a protein containing a disulfide bond [7–10]. The proposed mechanism involves mixed glutathione disulfide formation coupled with association and dissociation of the catalytic zinc ion. In a similar example of a non-innocent ligand, S-hydroxymethylglutathione is oxidized by the zinc enzyme alcohol dehydrogenase to S-formylglutathione (Scheme 1) [11].

The dielectric properties of the protein and electrostatic screening of zinc sites also affect the reactivity as does the redox potential of the Zn/S site [12,13]. Because entropic factors have a great influence on the redox potential of thiol/disulfide pairs, the zinc ion is an important determinant of the redox potential. As a result, the redox potential shifts to such a low value that mild cellular oxidants such as glutathione disulfide react with Zn/S sites and release Zn^{2+} [14]. This ligand-centered redox process can also lead to the release of cadmium(II) and copper(I) when these metal ions bind to metallothioneins under specific conditions [15].

In the context of on-going interest in the synthetic analogues of zinc proteins [3,16–25], we report the syntheses, spectral characterizations and structures of two tetradentate Schiff base ligands **L**^{1} and **L**^{2} (Scheme 2) and the products of these ligands reactions with Zn^{2+} in alcoholic media, $Zn^{II}(L^3)_2$ (**1**) and $Zn^{II}(L^4)_2$ (**2**). These products are the Zn^{II} complexes of the (NS) bidentate Schiff base ligands **L**^{3} and **L**^{4} (Scheme 3) formed by the reductive cleavage of the disulfide bond of **L**^{1} and **L**^{2} respectively. The direct synthesis of $Zn^{II}(L^3)_2$ from the thiol ligand, N-trans-cinnamylidene-2-mercaptoaniline, has been previously reported, but without a concomitant X-ray crystal structure [26]. We also discuss the prospective mechanism of the disulfide to thiolate transformation promoted by the Zn^{2+} centers.

* Corresponding author. Tel.: +98 311 391 3264; fax: +98 311 391 2350.
E-mail address: amirnasr@cc.iut.ac.ir (M. Amirnasr).

0277-5387/$ - see front matter © 2014 Elsevier Ltd. All rights reserved.
http://dx.doi.org/10.1016/j.poly.2013.12.040

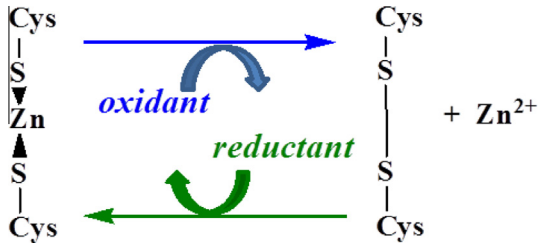

Scheme 1. Cartoon illustrating how a $Zn^{II}(Cys^{-})_2$ motif can display redox activity.

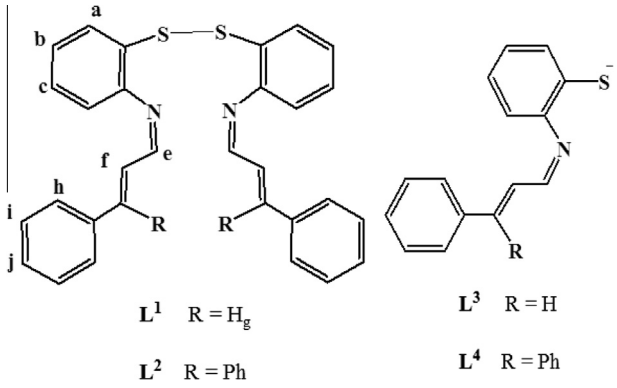

Scheme 2. The chemical formula of the Schiff base ligands $\mathbf{L^1}$, $\mathbf{L^2}$, $\mathbf{L^3}$ and $\mathbf{L^4}$.

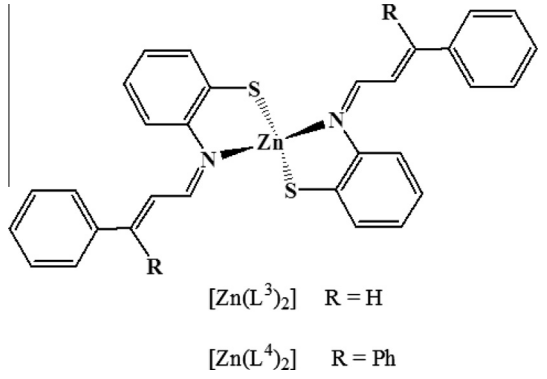

Scheme 3. The chemical formula of $[Zn(L^3)_2]$ and $[Zn(L^4)_2]$.

2. Experimental

2.1. Materials and general methods

All solvents and chemicals were of commercial reagent grade and were used as received from Aldrich and Merck. The Schiff base ligand $\mathbf{L^1}$ was prepared as reported elsewhere [27]. Infrared spectra from KBr pellets were collected on a FT-IR JASCO 680 plus spectrophotometer in the range 4000–400 cm^{-1}. UV–Vis absorption spectra were recorded on a JASCO V-570 spectrophotometer. ^1H NMR spectra were measured with a Bruker AVANCE III 400 spectrometer (400 MHz). Proton chemical shifts are reported in ppm relative to Me_4Si as internal standard. Elemental analyses were performed by using a Perkin–Elmer 2400II CHNS–O elemental analyzer. GC/MS analysis was performed with GC–MS-Agilent 5975C.

Electrochemical properties of these compounds were studied by cyclic voltammetry. Cyclic voltammograms were recorded by using a SAMA 500 Research Analyzer using a three electrode system, a glassy carbon working electrode (Metrohm 6.1204.110 with 2.0 ± 0.1 mm diameter), a platinum disk auxiliary electrode and Ag wire as reference electrode. CV measurements were performed in CH_3OH with lithium perchlorate as supporting electrolyte. The solutions were deoxygenated by purging with Ar for 5 min. All electrochemical potentials were calibrated versus internal $Fc^{+/0}$ (E^0 = 0.431 V versus SCE) couple under the same conditions [28].

2.2. Synthesis of ligands $\mathbf{L^1}$ and $\mathbf{L^2}$

The ligand $\mathbf{L^1}$ was prepared according to the literature [27] in 90% yield. *Anal.* Calc. for $C_{30}H_{24}N_2S_2$: C, 75.59; H, 5.08; N, 5.88; S, 13.45. Found: C, 75.20; H, 5.01; N, 5.95; S, 13.60%. FT-IR (KBr, cm^{-1}) ν_{max}: 1624 s (C=N). UV–Vis: λ_{max} (nm) (ε, L mol^{-1} cm^{-1}) ($CHCl_3$). 353 (18160), 294 (57840). ^1H NMR ($CDCl_3$, 400 MHz): δ = 7.02 (dd, J = 6.8, 1.6 Hz, 2H, H_a), 7.17–7.24 (m, 8H, $H_{b,c,d,g}$), 7.39–7.46 (m, 6H, $H_{i,j}$), 7.59 (dd, J = 8, 1.6 Hz, 4H, H_h), 7.66 (dd, J = 7.6, 1.6 Hz, 2H, H_f), 8.31 (dd, J = 6.8, 1.6 Hz, 2H, H_e).

The ligand $\mathbf{L^2}$ was synthesized by adding a solution of β-phenylcinnamaldehyde (0.416 g, 2 mmol) in methanol (2 mL) to a stirring solution of bis(2-aminophenyl)disulfide (0.250 g, 1 mmol) in methanol (5 mL). The mixture was stirred for 10 h to give a yellow precipitate. The product was filtered off and washed with cold methanol. Yield 93%; *Anal.* Calc. for $C_{42}H_{32}N_2S_2$: C, 80.22; H, 5.13; N, 4.45; S, 10.20. Found: C, 80.06; H, 5.02; N, 4.57; S, 10.05%. FT-IR (KBr, cm^{-1}) ν_{max}: 1605 s (C=N). UV–Vis: λ_{max} (nm) (ε, L mol^{-1} cm^{-1}) ($CHCl_3$): 367 (21650), 316 (42980). ^1H NMR ($CDCl_3$, 400 MHz): δ = 6.79 (m, 2H, H_a), 7.11 (m, 4H, $H_{b,c}$), 7.19 (d, J = 9.2 Hz, 2H, H_d), 7.34–7.47 (m, 20H, $H_{i,j,h}$), 7.60 (m, 2H, H_f), 8.16 (d, J = 9.2 Hz, 2H, H_e.

2.3. Synthesis of $[Zn(L^3)_2]$ (**1**)

To a solution of $Zn(OAc)_2.2H_2O$ (22 mg, 0.1 mmol) in methanol (10 mL) was added a solution of $\mathbf{L^1}$ (47.6 mg, 0.1 mmol) in $CHCl_3$ (10 mL), and the mixture was stirred at room temperature for two days to give a clear orange solution. Orange single crystals of complex **1** suitable for X-ray crystallography were obtained by slow evaporation of solvents. Yield 57%. *Anal.* Calc. for $C_{30}H_{24}N_2S_2Zn$: C, 66.47; H, 4.46; N, 5.17; S, 11.83. Found: C, 65.87; H, 4.25; N, 5.38; S, 11.68%. FT-IR (KBr, cm^{-1}) ν_{max}: 1616 s (C=N). UV–Vis: λ_{max} (nm) (ε, L mol^{-1} cm^{-1}) ($CHCl_3$): 459 (7790), 341 (32,760). ^1H NMR ($CDCl_3$, 400 MHz): δ = 7.01–7.54 (m, 20H, $H_{a,b,c,d,g,h,i,j}$), 7.88 (d, J = 7.6 Hz, 2H, H_f), 8.61 (d, J = 10 Hz, 2H, H_e).

2.4. Synthesis of $[Zn(L^4)_2]$ (**2**)

The complex **2** was prepared by a procedure similar to that of **1** except that $\mathbf{L^2}$ (62.9 mg, 0.1 mmol) was used instead of $\mathbf{L^1}$. Orange crystals were collected by filtration and washed with small amounts of methanol. Yield 37%. *Anal.* Calc. for $C_{42}H_{32}N_2S_2Zn$: C, 72.66; H, 4.65; N, 4.04; S, 9.24. Found: C, 71.31; H, 4.87; N, 4.18; S, 9.22%. FT-IR (KBr, cm^{-1}) ν_{max}: 1604 s (C=N). UV–Vis: λ_{max} (nm) (ε, L mol^{-1} cm^{-1}) ($CHCl_3$) 475 (1825), 321 (38,522). ^1H NMR ($CDCl_3$, 400 MHz): δ = 6.84–7.42 (m, 28H, $H_{aromatic}$), 7.65 (dd, J = 8, 1.2 Hz, 2H, H_f), 8.38 (d, J = 10 Hz, 2H, H_e).

2.5. Crystal structure determination and refinement for **1** and **2**

Orange single crystals of **1** and **2** were obtained by slow evaporation of a methanol solution of **1**, and a dichloromethane-methanol solution of **2** (2.5:1 v/v) at room temperature. **2** crystallized as a solvate incorporating obviously both solvents in a slightly disordered and non-stoichiometric fashion. Due to the very small size of the available crystals the diffraction data of **1** were collected at the ESRF with a synchrotron source (λ = 0.70135 Å) at T = 100 K and a diffractometer with a Dectris Pilatus 2 M pixel

detector. Cell refinement, data reduction and correction for absorption (multi-scan method) were performed with instrument software [29]. The structure was solved with direct methods using the program SIR2004 [30] and structure refinement on F^2 was carried out with the program SHELXL97 [31].

X-ray data for **2** were collected at $T = 100$ K on a Bruker Kappa APEX-2 CCD diffractometer with graphite monochromated Mo Kα ($\lambda = 0.71073$ Å) radiation. Cell refinement and data reduction were performed with program SAINT [32]. Correction for absorption was carried out with the multi-scan method and program SADABS [32]. The structure was solved with direct methods using the program SHELXS97 and structure refinement on F^2 was carried out with the program SHELXL97 [31]. A dichloromethane solvent molecule disordered about a symmetry center at $x, y, z = ½, ½, 0$ and obviously intermingled with methanol was taken into account by refining the population parameters of one chlorine and one carbon atom position without restraints and neglecting any hydrogen atoms. The final population factors for these two sites were Cl1s 0.387(4) and C1s 0.472(15) (distances C1s–Cl1s 1.68 and 1.83 Å, C1s···C1s 1.99 Å, Cl1s···Cl1s 2.89 Å; Cl1s–C1s–Cl1s 111°). The chemical formula of the solid, $C_{42}H_{32}N_2S_2Zn{\cdot}0.5(CH_2Cl_2)$ (Table 1), is idealized and would require population factors of 1 for Cl1s and 0.5 for C1s. A summary of important crystallographic data, data collection and refinement details is presented in Table 1. Structural diagrams (see below) were created with program DIAMOND [33].

3. Results and discussion

3.1. Synthesis and characterization

The tetradentate N_2S_2 donor Schiff-base ligands $\mathbf{L^1}$ and $\mathbf{L^2}$ were prepared by the condensation of the corresponding aldehydes with bis(2-aminophenyl)disulfide in 2:1 M ratio in methanol. The products precipitated and were readily isolated in approximately 90% and 93% yield respectively. The ligands were characterized by CHN analysis and different spectroscopic methods.

The Zn(II) complexes **1** and **2** (Scheme 3) were synthesized in methanol solution by the reaction of $Zn(OAc)_2{\cdot}2H_2O$ and disulfide Schiff base ligands $\mathbf{L^1}$ or $\mathbf{L^2}$, respectively, in a 1:1 M ratio. Notably, in each case, the disulfide ligand is reduced to two thiolate NS ligands in the presence of Zn(II) (Scheme 4).

This reaction was carried out in several alcohols including methanol, ethanol and n-propanol. When n-propanol was used as the solvent, the reducing role of alcohol was confirmed by the detection of propionaldehyde as a reaction product by gas chromatography-mass spectrometry (molecular ion $(M)^+$ at $m/z = 58.1$). Since the ligand $\mathbf{L^1}$ is stable in these solvents, zinc acetate must be facilitating the reduction of the disulfide to thiolate with concomitant oxidation of the alcohol.

The reaction is also facilitated by a base such as triethylamine (Fig. 1). The visible absorption spectrum of $Zn(L^3)_2$ in methanol solvent shows a maximum at 446 nm (Fig. 1a). When equal volumes of $Zn(OAc)_2$ (2×10^{-4} M) in methanol and $\mathbf{L^1}$ (2×10^{-4} M) in chloroform were mixed, absorbance changes at 446 nm indicating the formation of $Zn(L^3)_2$ occurred much more rapidly in the presence of added Et_3N (10^{-3} M) than in its absence (Fig. 1b). This suggests that the added Et_3N acts as proton scavenger in this process. It is likely that the acetate counterion added with the zinc also serves this purpose.

3.2. Description of the crystal structures of *1* and *2*

The crystal structure of the ligand $\mathbf{L^1}$ has been reported previously [27]. By means of an independent X-ray structure determination (results available upon request) we were able to confirm this result and proved that our $\mathbf{L^1}$ material is the disulfide Schiff base ligand shown in Scheme 2. According to [27], bond lengths and angles in the central C–S–S–C group of $\mathbf{L^1}$ are S–S = 2.0302(6) Å, C–S = 1.782(2) and 1.779(2) Å, and C–S–S–C = −86.14(8)° at 100 K, while our own values were similar but obtained at room temperature.

Compound **1**, $[Zn(L^3)_2]$, crystallizes in monoclinic space group $C2/c$. The molecular structure is shown in Fig. 2, and selected bond distances and angles are listed in Table 2. This structure clearly shows that the ligand $\mathbf{L^1}$ has undergone scission of the disulfide bond to give two NS bidentate thiolate Schiff base ligands coordinated to the Zn(II). The angles around the metal center deviate significantly from the 109.5° of an ideal tetrahedron and range from 88.82(5)° for N1–Zn–S1 to 127.10(3)° for S2–Zn–S1. The average bond lengths of 2.081 Å for Zn–N and of 2.276 Å for Zn–S agree well with the analogous distances reported for related tetrahedral zinc complexes [3,34–36]. The S···S distance in the tetrahedron is 4.075 Å, about twice the length of the S–S bond in $\mathbf{L^1}$. The complex $[Zn(L^3)_2]$ obeys nicely a non-crystallographic molecular symmetry 2-C_2. Compared with $\mathbf{L^1}$ [27], the C–S bonds in $[Zn(L^3)_2]$ are shorter by ca. 0.025 Å while the C–N bonds are longer on average by 0.016 Å, in qualitative agreement with expectation. On transition from $\mathbf{L^1}$ [27] to $[Zn(L^3)_2]$ a larger alteration affects intramolecular S···N distances, which increase from 2.80 Å in $\mathbf{L^1}$ to 3.05 Å in $[Zn(L^3)_2]$ by an in-plane repositioning of the S atoms relative to the almost rigid aminobenzene fragments.

The molecular structure of **2** is shown in Fig. 3, and selected bond distances and angles are listed in Table 2. This complex crystallizes in triclinic space group $P\bar{1}$. Again, the Schiff base ligand, $\mathbf{L^2}$ has undergone scission of the disulfide bond to two NS bidentate thiolate ligands. The coordination geometry around the Zn(II) center is distorted tetrahedron with angles ranging from 88.81(6)° for N2–Zn1–S2 to 132.09(3)° for S2–Zn1–S1. The mean bond lengths of Zn–N = 2.087 Å and Zn–S = 2.266 Å are similar to $[Zn(L^3)_2]$ and in agreement with corresponding distances reported for related

Table 1
Crystallographic parameters, data collection and refinement details for $[Zn(L^3)_2]$ and $[Zn(L^4)_2]$.

Compound	$[Zn(L^3)_2]$	$[Zn(L^4)_2]$
Empirical Formula	$C_{30}H_{24}N_2S_2Zn$	$C_{42}H_{32}N_2S_2Zn{\cdot}0.5(CH_2Cl_2)$
Formula weight	542.00	736.65
T (K)	100(2)	100(2)
Crystal system	monoclinic	triclinic
Space group	$C2/c$	$P\bar{1}$
a (Å)	32.1293(7)	12.3544(4)
b (Å)	7.96002(12)	13.1530(4)
c (Å)	20.3490(5)	13.3605(4)
α (°)	90.00	100.860(2)
β (°)	102.281(2)	113.970(2)
γ (°)	90.00	111.234(2)
V (Å^3)	5085.17(19)	1699.58(9)
Z	8	2
D_{calc} (Mg/m^3)	1.419	1.439
μ (mm^{-1})	1.04	0.96
Crystal size (mm)	0.3 × 0.02 × 0.01	0.16 × 0.14 × 0.11
F(000)	2240	762
θ range(°)	2.0–26.6	1.9–27.0
Absorption correction	empirical	multi-scan
Reflections collected	5429	24235
R_{int}	0.0586	0.051
Data/restraints/parameters	5429/0/316	7409/0/444
Goodness-of-fit (GOF) on F^2	1.035	1.022
Final R indices $[I > 2\sigma(I)]$[a]	$R_1 = 0.045$, $wR_2 = 0.135$	$R_1 = 0.043$, $wR_2 = 0.107$
Largest difference in peak and hole (e Å^{-3})	1.46 and −0.46	0.43 and −0.56

[a] $R_1 = \sum||F_o| - |F_c||/\sum|F_o|$, $wR_2 = \{\sum[w(F_o^2 - F_c^2)^2]/\sum[w(F_o^2)^2]\}^{1/2}$.

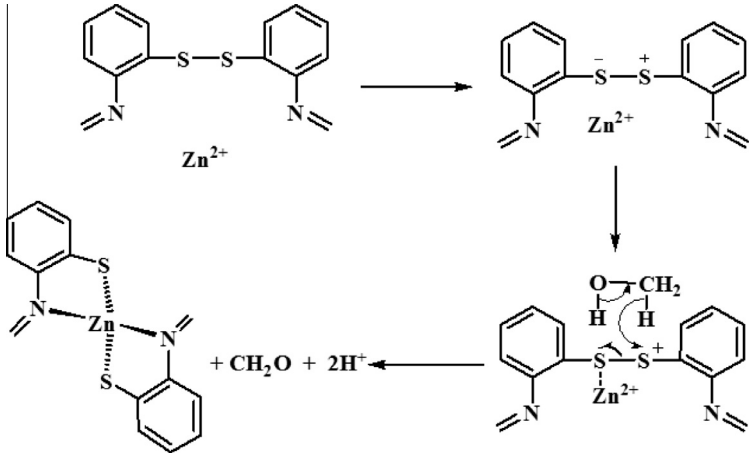

Scheme 4. Proposed reaction mechanism for reductive S–S bond cleavage in MeOH.

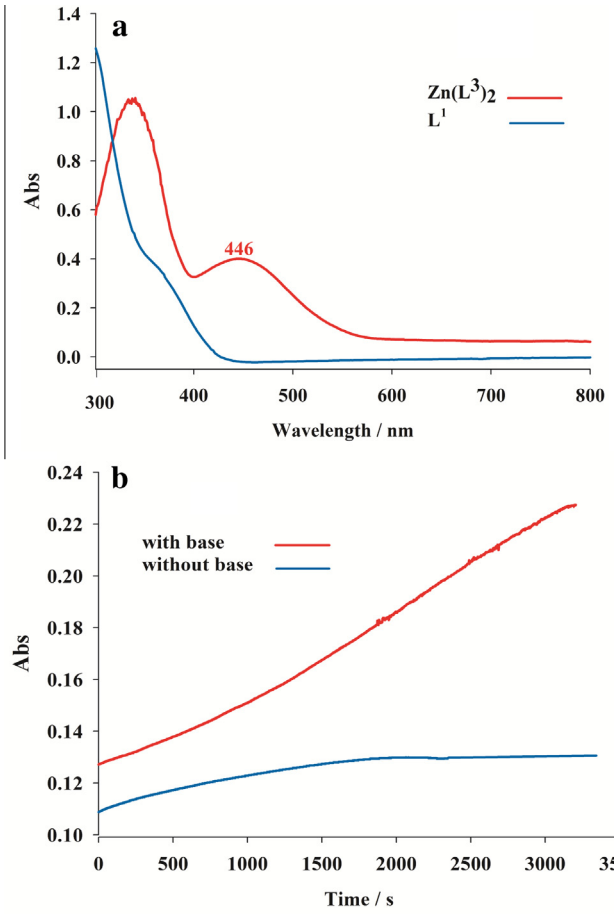

Fig. 1. a) Electronic absorption spectra of $\mathbf{L^1}$ (blue) and $Zn(L^3)_2$ (red) in methanol; b) Temporal absorbance changes at 446 nm in the absence (blue) and presence of added base, Et_3N, (red). (Color Online.)

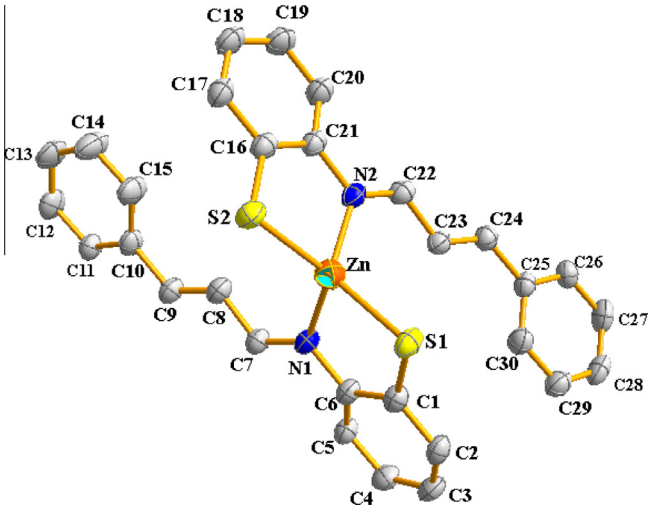

Fig. 2. The molecular structure of $[Zn(L^3)_2]$ with its atom labelling scheme. Displacement ellipsoids are drawn at 50% probability.

Table 2
Selected bond lengths (Å) and angles (°) for $[Zn(L^3)_2]$ and $[Zn(L^4)_2]$.

$[Zn(L^3)_2]$		$[Zn(L^4)_2]$	
Bond lengths			
Zn–N1	2.079(2)	Zn1–N1	2.085(2)
Zn–N2	2.083(2)	Zn1–N2	2.090(2)
Zn–S1	2.2778(6)	Zn1–S1	2.2687(7)
Zn–S2	2.2738(7)	Zn1–S2	2.2644(8)
Bond angles			
N1–Zn–N2	108.60(8)	N1–Zn1–N2	109.88(8)
N1–Zn–S2	122.80(6)	N1–Zn1–S2	119.00(6)
N2–Zn–S2	89.01(6)	N2–Zn1–S2	88.81(6)
N1–Zn–S1	88.82(5)	N1–Zn1–S1	89.10(6)
N2–Zn–S1	122.40(6)	N2–Zn1–S1	118.98(6)
S2–Zn–S1	127.10(3)	S2–Zn1–S1	132.09(3)

zinc complexes [3,34–36]. Further geometric trends outlined for $[Zn(L^3)_2]$ are valid also for $[Zn(L^4)_2]$.

3.3. Spectral characterization

Both **1** and **2** are air-stable solids and have good elemental analyses. The FT-IR spectra of the free ligands $\mathbf{L^1}$ and $\mathbf{L^2}$ exhibit the characteristic imine C=N bands at 1624 and 1605 cm^{-1}, respectively. Similar features are observed in the FT-IR spectra of **1** and **2**, with the C=N stretching vibrations appearing at 1616 and 1604 cm^{-1} respectively.

The UV–Vis data of $\mathbf{L^1}$, $\mathbf{L^2}$ and the Zn(II) complexes **1** and **2** in $CHCl_3$ are presented in the Experimental Section. The electronic absorption spectra of the two ligands in chloroform consists of relatively intense bands centered at 294 nm for $\mathbf{L^1}$ and at 316 nm for $\mathbf{L^2}$, assigned to π–π^* transitions. A second band at 353 nm for $\mathbf{L^1}$

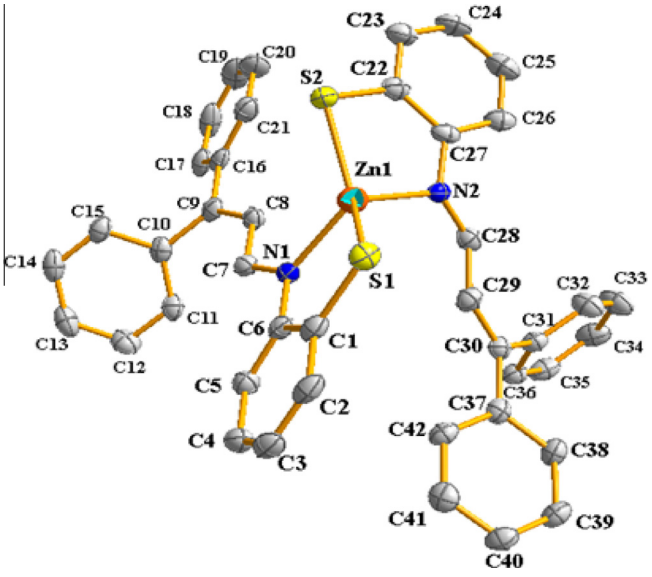

Fig. 3. The molecular structure of $[Zn(L^4)_2]$ with its atom labelling scheme. Displacement ellipsoids are drawn at 50% probability.

and 367 nm for $\mathbf{L^2}$, corresponds to the n–π^* transition. Complex **1** shows two bands at 459 and 341 nm, assigned to the intraligand transitions. The complex **2** also shows intraligand transitions at 475, 360, and 321 nm. As in related d^{10} metal complexes, no d-d transition would be expected for these compounds [37].

The ^{1}H NMR spectroscopic data recorded in $CDCl_3$ solution for $\mathbf{L^1}$ and $\mathbf{L^2}$ and for **1** and **2** are reported in the Experimental Section The main feature of the ^{1}H NMR spectra of these compounds is the signal due to the CH_{imine} group. This signal appears at 8.30, 8.15, 8.6 and 8.38 ppm for $\mathbf{L^1}$, $\mathbf{L^2}$, **1** and **2** respectively. The aromatic protons of these compounds appear in the appropriate region (5.8–7.8 ppm) [26,38].

3.4. Electrochemical studies

To verify the effect of Zn(II) on the reduction of the S-S bond the electrochemical behavior of $\mathbf{L^1}$ in the absence and presence of Zn(II) was investigated by cyclic voltammetry. The cyclic voltammograms of $\mathbf{L^1}$ and $\mathbf{L^1}$ + Zn(II) in methanol are presented in Fig. 4. The ligand-centered irreversible reduction observed at −1.25 V (blue CV) corresponds to the reduction of S–S bond of the free ligand $\mathbf{L^1}$, and is in agreement with the reduction of closely related disulfide Schiff bases reported in the literature [39]. In the presence of equimolar zinc acetate this reduction process occurs at −0.98 V. The 0.27 V shift to less negative potentials is presumably due to the polarization of the S–S bond of $\mathbf{L^1}$ induced by Zn(II) ion, and gives further support to the S–S bond cleavage by the model presented in Scheme 4. The irreversible reduction wave at −1.48 V corresponds to Zn(II)/Zn(0) of $Zn(L^3)_2$, produced after the first reduction process. A similar reduction wave is observed in the CV of complex **1**, $Zn(L^3)_2$, in methanol solution (Fig. 5).

4. Theoretical calculations

Theoretical calculations were performed in order to rationalize the S–S bond cleavage observed upon the formation of **1**, from zinc acetate and $\mathbf{L^1}$. First, the structure of the $[Zn(L^3)_2]$ complex was optimized in the gas phase at the Hartree–Fock (HF) level of theory using 6-31G(d) basis set on the C, N, H and S atoms, and the relativistic effective core pseudo potential LANL2DZ for the zinc atom. The optimized HF structure was used as the starting geometry for

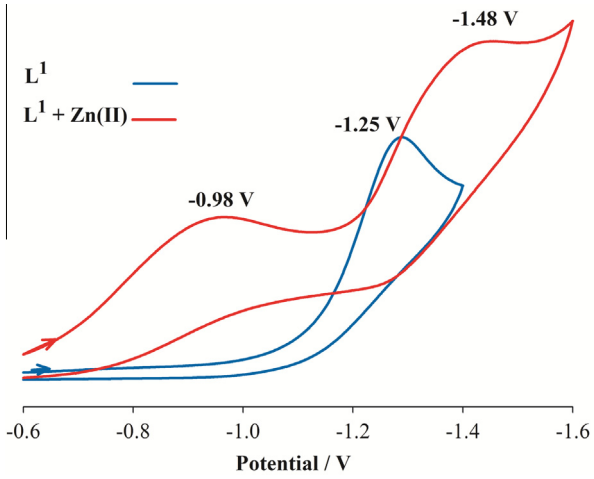

Fig. 4. Cyclic voltammogram of $\mathbf{L^1}$ in methanol, in the absence (blue) and presence of Zn(II) (red), T = 298 K, $c = 1 \times 10^{-3}$ M. Scan rate = 100 mV s^{-1}. (Color Online.)

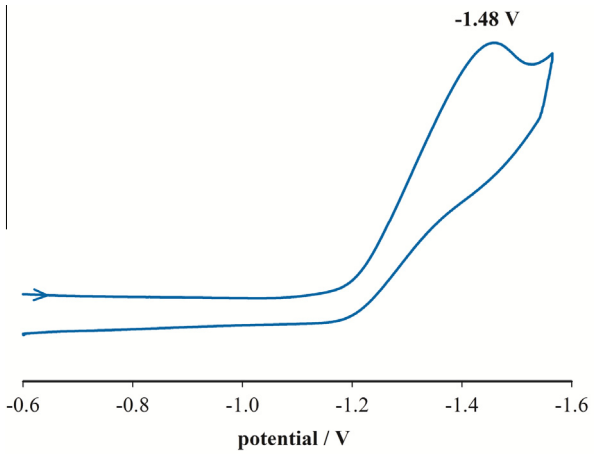

Fig. 5. Cyclic voltammogram of complex **1**, $[Zn(L^3)_2]$, in methanol. T = 298 K, $c \approx 1 \times 10^{-3}$ M. Scan rate = 100 mV s^{-1}.

the optimization at the DFT-B3LYP level of theory. The basis set for the C, N, H and S atoms were improved to the 6-311++G(d,p) and again LANL2DZ was used for the Zn atom. Vibrational frequency calculations were performed on the optimized structure of the complex to search for the imaginary frequency and obtain the vibrational frequencies of complex in the gas phase. The optimized structure did not show any imaginary vibrational frequency which confirms that the optimized structure is at a local minimum. The structure obtained from geometry optimization conforms approximately to the distorted tetrahedral geometry around the Zn atom determined by X-ray diffraction analysis. A comparison of calculated and experimental values of selected bond length and angles of **1** is provided in Table 3.

Table 3
Selected experimental vs. calculated bond lengths (Å) and angles (°) of $[Zn(L^3)_2]$.

	Theoretical	Experimental
Zn–N1, Zn–N2	2.167 (2×)	2.079(2), 2.083(2)
Zn–S1, Zn–S2	2.406 (2×)	2.278(6), 2.274(7)
N1–Zn–N2	108.07	108.60(8
S1–Zn–S2	137.26	127.10(3)
N1–Zn–S1, N2–Zn–S2	85.54 (2×)	88.82(5), 89.01(6)
N1–Zn–S2, N2–Zn–S1	120.38 (2×)	122.80(6), 122.40(6)

Assignment of the IR spectrum of **1** can be proposed on the basis of frequency agreement between the computed harmonics and the observed fundamental modes (see the Supporting information). The small differences between the calculated and experimental vibrational frequencies are likely to originate from (i) the environmental conditions (solvent effect) and (ii) from the fact that the experimental values are anharmonic frequencies while the calculated values are harmonic.

As described above, the solvent alcohol apparently serves as the reducing agent in the process leading to the reduction of the disulfide bond to thiolate in the presence of Zn(II). Thus, it is of interest to theoretically find a transition state (TS) that might represent the Zn^{2+} mediated reduction of the disulfide bond by the solvent. To pursue this goal, the semi-empirical PM6 method, containing the Zn, C, S, N and H parameters, was used. Several initial structures containing the ligand, Zn^{2+} ion and a molecule of solvent (MeOH) were proposed (e.g., Fig. 6) and the computational method led to the transition state (TS) presented showing transfer of hydride from MeOH to the S atom of the ligand and simultaneous breaking of the S–S bond. To facilitate the TS searching, the size of the ligand was reduced and the Zn^{2+} ion was initially positioned at nearly equal distances from S and N atoms. The transition state optimization (opt = modredundant, calcfc, noeigen, TS) of the initial structure (Fig. 6) at the PM6 level of theory converged to the TS structure shown in Fig. 7.

The unrestricted HF frequency calculations on the optimized structure of TS at the PM6 level of theory found one imaginary frequency. The vibrational frequency is about $-1060.82\ cm^{-1}$. The majority of the motion in this mode involves shifting the hydrogen atom from the C atom of CH_3OH to the S atom of the ligand and also vibration in the S–S bond. As evident from Fig. 7, the distance between the C and H is increased and the H atom is getting close to the S atom. The C–H bond distance in the free methanol is about 1.07 Å. It is increased to 1.86 Å in the TS and shows that the C–H bond is breaking. The value of the S–H bond distance in the TS is 1.39 Å which is very close to the corresponding value in H_2S molecule (1.31 Å) and confirms that the S–H bond is forming. The S–S bond distance in the TS is about 2.218 Å which is larger than the corresponding value in the free ligand (2.07 Å) indicating the tendency of this bond toward breaking. The most interesting point is that the bond order of the C–O bond increases in the TS relative to the free CH_3OH molecule. The C–O bond distance in TS is 1.29 Å which is smaller than the corresponding value in free CH_3OH molecule (1.43 Å) and close to the C–O bond distance (1.225 Å) in formaldehyde [40]. This observation confirms that the methanol is oxidized to the formaldehyde in this reaction, which is in accord with the experimental results reported above.

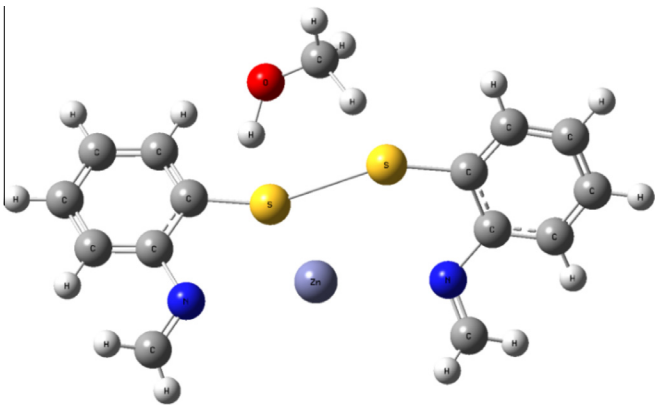

Fig. 6. The initial structure which leads to the relatively correct structure for the TS.

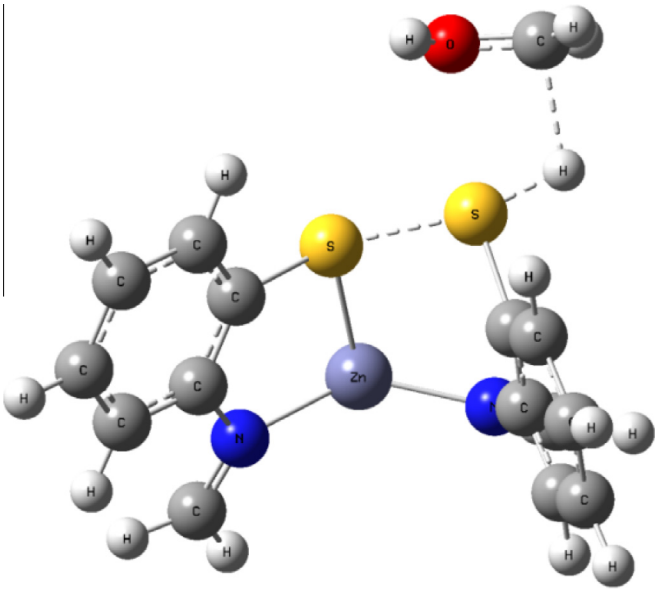

Fig. 7. The optimized transition state in the Zn assisted reductive S–S bond cleavage of the model complex for $[Zn(L^3)_2]$ and $[Zn(L^4)_2]$ in the presence of methanol at the PM6 level of theory.

5. Conclusion

In this work, we have reported the synthesis of two disulfide Schiff base ligands. The reaction of the disulfide ligands, $\mathbf{L^1}$ and $\mathbf{L^2}$, with Zn(II) in alcoholic solvents leads to the reductive cleavage of the S–S bond and formation of $Zn(NS)_2$ complexes in a process relevant to analogous processes seen with zinc finger proteins. In essence, we have described a very simple method for clean reductive cleavage of the disulfide bond under mild conditions that could be used as a model of zinc coordination environments in proteins.

The reaction is also facilitated by a base which consumes the protons released in the redox process, shifting the reaction to the zinc thiolate complex formation.

Acknowledgements

Partial support of this work by the Isfahan University of Technology Research Council is gratefully acknowledged. Aspects of this work were carried out at UCSB under the sponsorship of the US National Science Foundation Grant CHE-0749524. We further thank the Swiss Norwegian Beam Line at the ESRF for the data collection of one compound.

Appendix A. Supplementary data

CCDC 920963 and 929027 contains the supplementary crystallographic data for **1** and **2**. These data can be obtained free of charge via http://www.ccdc.cam.ac.uk/conts/retrieving.html, or from the Cambridge Crystallographic Data Centre, 12 Union Road, Cambridge CB2 1EZ, UK; fax: (+44) 1223-336-033; or e-mail: deposit@ccdc.cam.ac.uk. Supplementary data associated with this article can be found, in the online version, at http://dx.doi.org/10.1016/j.poly.2013.12.040.

References

[1] M. Vasak, G. Meloni, J. Biol. Inorg. Chem. 16 (2011) 1067.
[2] W. Maret, J. Biol. Inorg. Chem. 16 (2011) 1079.

[3] S. Atrian, M. Capdevila, BioMol Concepts 4 (2013) 143.
[4] T. Fukada, S. Yamasaki, K. Nishida, M. Murakami, T. Hirano, J. Biol. Inorg. Chem. 16 (2011) 1123.
[5] D.S. Auld, Biometals 14 (2001) 271.
[6] W. Maret, B.L. Vallee, Proc Natl. Acad. Sci. USA 95 (1998) 3478.
[7] A. Krężel, W. Maret, Biochem. J. 402 (2007) 551.
[8] M. Papworth, P. Kolasinska, M. Minczuk, Gene 366 (2006) 27.
[9] C.S. Sevier, C.A. Kaiser, Mol. Cell Biol. 3 (2002) 836.
[10] R.A. Kumar, A. Koc, R.L. Cerny, V.N. Gladyshev, J. Biol. Chem. 277 (2002) 37527.
[11] I. Dalle-Donne, D. Giustarini, R. Colombo, A. Milzani, R. Rossi, Free Radical Biol. Med. 38 (2005) 1501.
[12] I.A. Topol, C. McGrath, E. Chertova, C. Dasenbrock, W.R. Lacourse, M.A. Eissenstat, S.K. Burt, L.E. Henderson, J.R. Casas-Finet, Prot. Sci. 10 (2001) 1434.
[13] A.T. Maynard, D.G. Covell, J. Am. Chem. Soc. 123 (2001) 1047.
[14] W. Maret, Proc. Natl. Acad. Sci. USA 91 (1994) 237.
[15] R.R. Misra, J.F. Hochadel, M.P. Waalkes, G.T. Smith, D.A. Wink, J.C. Cook, M.P. Waalkes, D.A. Wink, Chem. Res. Toxicol. 9 (1996) 326.
[16] K. Singh, M.S. Barwa, P. Tyagi, Eur. J. Med. Chem. 42 (2007) 394.
[17] E. Canpolat, M. Kaya, J. Coord. Chem. 57 (2004) 1217.
[18] M. Yildiz, B. Dulger, S.Y. Koyuncu, B.M. Yapici, J. Indian Chem. Soc. 81 (2004) 7.
[19] A. Prakash, D. Adhikari, Int. J. Chem. Technol. Res. 3 (2011) 1891.
[20] R. Vogler, M. Gelinsky, L.F. Guo, H. Vahrenkamp, Inorg. Chim. Acta 339 (2002) 1.
[21] M. Rombach, M. Gelinsky, H. Vahrenkamp, Inorg. Chim. Acta 334 (2002) 25.
[22] S. Ranganathan, K.M. Muraleedharan, P. Bharadwaj, D. Chatterji, I. Karle, Tetrahedron 58 (2002) 2861.
[23] M. Ji, H. Vahrenkamp, Eur. J. Inorg. Chem. (2005) 1398.
[24] E. Almaraz, Q.A. de Paula, Q. Liu, J.H. Reibenspies, M.Y. Darensbourg, N.P. Farrell, J. Am. Chem. Soc. 130 (2008) 6272.
[25] O.P. Anderson, A. Cour, M. Findeisen, L. Hennig, O. Simonsen, L.F. Taylor, H. Toftlund, J. Chem. Soc., Dalton Trans. (1997) 111.
[26] N. Ancin, S. Ide, S.G. Öztas, M. Tüzün, E. Sahin, J. Mol. Struct. 608 (2002) 89.
[27] J. Raftery, S. Jhaumeer-Laulloo, M.G. Bhowon, K. Chikhooree, J.A. Joule, Acta Crystallogr., Sect. E 66 (2010) o3307.
[28] J. Reiter, J. Vondrák, F. Opekar, M. Sedlaříková, J. Velická, B. Klápště, in: Meeting Abstracts of the 12th International Meeting on Lithium Bateries, Nara, Japan 2004, Abstract No. 237.
[29] MAR research programs mar345dtb and automar. Marresearch GmbH, Norderstedt, Germany.
[30] M.C. Burla, R. Caliandro, M. Camalli, B. Carrozzini, G.L. Cascarano, L. De Caro, C. Giacovazzo, G. Polidori, R. Spagna, J. Appl. Crystallogr. 38 (2005) 381.
[31] G.M. Sheldrick, Acta Crystallogr., Sect. A 64 (2008) 112.
[32] Bruker computer programs APEX2, SAINT, and SADABS. Bruker AXS Inc., Madison, Wisconsin, USA, 2008.
[33] K. Brandenburg, M. Berndt, J. Appl. Crystallogr. 32 (1999) 1028.
[34] J.S. Figueroa, K. Yurkerwich, J. Melnick, D. Buccella, G. Parkin, Inorg. Chem. 46 (2007) 9234.
[35] J. Schnödt, M. Sieger, T. Schleid, I. Hartenbach, W. Kaim, Z. Anorg. Und Allg. Chem. 636 (2010) 385.
[36] K. Boerzel, H. Koeckert, M. Bu, W. Spingler, S.J.B. Lippard, Inorg. Chem. 42 (2003) 1604.
[37] K. Grubel, K. Rudzka, A.M. Arif, K.L. Klotz, J.A. Halfen, L.M. Berreau, Inorg. Chem. 49 (2010) 82.
[38] S. Meghdadi, M. Amirnasr, K.J. Schenk, S. Dehghanpour, Helv. Chim. Acta 85 (2002) 2807.
[39] G.V. Loukova, A.D. Garnoveskii, Russ. Chem. Bull. 48 (1999) 1503.
[40] A.F. Wells, Structural Inorganic Chemistry, fifth ed. Clarendon Press, Oxford, UK.